Alterations in Muscle Networks in the Upper Extremity of Chronic Stroke Survivors

Michael Houston, Xiaoyan Li, Ping Zhou, *Senior Member, IEEE*, Sheng Li, Jinsook Roh, and Yingchun Zhang, *Senior Member, IEEE*

***Abstract*— Muscle networks describe the functional connectivity between muscles quantified through the decomposition of intermuscular coherence (IMC) to identify shared frequencies at which certain muscles are co-modulated by common neural input. Efforts have been devoted to characterizing muscle networks in healthy subjects but stroke-linked alterations to muscle networks remain unexplored. Muscle networks were assessed for eight key upper extremity muscles during isometric force generation in stroke survivors with mild, moderate, and severe impairment and compared against healthy controls to identify stroke-specific alterations in muscle connectivity. Coherence matrices were decomposed using non-negative matrix factorization. The variance accounted for thresholding was then assessed to identify the number of muscle networks. Results showed that the number of muscle networks decreased in stroke survivors compared to age-matched healthy controls (four networks in the healthy control group) as the severity of post-stroke motor impairment increased (three in the mild- and two in the moderate- and severe-stroke groups). Statistically significant reductions of IMC in the synergistic deltoid muscles in the alpha-band in stroke patients versus healthy controls ($p < 0.05$) were identified. This study represents the first effort, to the best of our knowledge, to assess stroke-linked alterations in functional intermuscular connectivity using muscle network analysis. The findings revealed a pattern of alterations to muscle networks in stroke survivors compared to healthy controls, as a result of the loss of brain function associated with the stroke. These alterations in muscle networks reflected underlying pathophysiology. These findings can help better understand the motor impairment and motor control in stroke and may advance rehabilitation efforts for stroke by identifying the impaired neuromuscular coordination among multiple muscles in the frequency domain.**

***Index Terms*— Muscle network, intermuscular coherence, muscle synergy, neuromuscular control, stroke.**

I. Introduction

STROKE is one of the leading causes of disabilities in the US [1], often leading to abnormal motor coordination with the muscles of the affected arm [2]–[4]. Previous studies have shown that the nervous and musculoskeletal systems work interactively to simplify neuromuscular control by simultaneously co-activating groups of muscles as motor building blocks, so-called muscle synergies, to reduce the degrees of freedom in the redundant musculoskeletal system [5]–[11]. The effects of stroke on intermuscular coordination have traditionally been studied with muscle synergy analysis [12]–[17] as well as intermuscular coherence (IMC) [18]–[20].

A variety of dimensionality reduction tools, including the non-negative matrix factorization (NNMF) [21], have been utilized to identify muscle synergies, the anatomical coordination of muscle activation. For example, alterations in the composition of muscle synergy patterns of isometric force generation have been identified by applying NNMF in chronic stroke patients with severe impairment, compared to age-matched healthy controls [16]. Abnormal co-activation of the anterior, middle, and posterior deltoid fibers was observed in the stroke patients whereas healthy controls exhibited co-activation of the anterior and middle deltoids in one synergy and co-activation of the middle and posterior deltoids in another synergy. In addition, the NNMF algorithm applied to the electromyographic (EMG) data collected from stroke survivors with varying levels of motor impairment identified that alterations in proximal muscle synergies were also evident in a lesser severity of stroke impairment, but still most pronounced in the severe stroke [17]. The alteration in the proximal muscle synergies implies a potential lack of ability for post-stroke survivors to selectively activate deltoid muscles under isometric conditions. However, while muscle synergies can represent the anatomical intermuscular coordination patterns in neuromuscular control, they cannot quantify the functional connectivity among muscles such as coherence can [22].

Manuscript received November 9, 2020; revised March 1, 2021 and April 1, 2021; accepted April 21, 2021. Date of publication April 26, 2021; date of current version June 9, 2021. This work was supported in part by the American Heart Association Scientist Development under Grant 17SDG33670561 and in part by the University of Houston. *(Corresponding authors: Yingchun Zhang; Jinsook Roh.)*

This work involved human subjects or animals in its research. Approval of all ethical and experimental procedures and protocols was granted by the Northwestern University Institutional Review Board and performed in line with the Declaration of Helsinki.

Michael Houston, Jinsook Roh, and Yingchun Zhang are with the Department of Biomedical Engineering, University of Houston, Houston, TX 77004 USA (e-mail: jroh@central.uh.edu; yzhang94@uh.edu).

Xiaoyan Li is with the Department of Physical Medicine and Rehabilitation, University of Texas Health Science Center at Houston, Houston, TX 77030 USA, and also with TIRR Memorial Hermann Hospital, Houston, TX 77030 USA.

Ping Zhou is with the Institute of Rehabilitation Engineering, The University of Rehabilitation, Qingdao 266000, China.

Sheng Li is with the Department of Physical Medicine and Rehabilitation, University of Texas Health Science Center at Houston, Houston, TX 77030 USA, also with TIRR Memorial Hermann Hospital, Houston, TX 77030 USA, and also with the Institute of Rehabilitation Engineering, The University of Rehabilitation, Qingdao 266000, China.

Digital Object Identifier 10.1109/TNSRE.2021.3075907

Coherence, a measure of the correlation between two signals in the frequency domain, can be used to assess the functional connectivity among muscles [23], [24]. Using IMC analysis, Kisiel-Sajewicz *et al.* discovered reduced functional coupling of the synergistic muscle pair of the anterior deltoid and triceps brachii muscles in the 0-11 Hz frequency range in severely impaired stroke participants compared to healthy controls [18]. The reduced functional connectivity revealed in the study for the synergistic muscle pairs in stroke participants may explain the poor motor control in target-reaching tasks in stroke, and could be further explained by the loss or reduction of the common neural input to the muscles, likely as a result of the damage to the cortico-spinal pathways. Fisher *et al.* also found that IMC of the first dorsal interosseous, extensor digitorum communis, and flexor digitorum superficialis muscles in the beta band (15-30 Hz) was associated with the integrity of the cortico-spinal tract [19].

Modulations of the neural input to muscles in specific frequency ranges have also been investigated using IMC or connectivity analysis. In one study involving hand muscles in two distinct pinch tasks, modulations of the oscillatory neural input were found as an increase at 10 Hz and a decrease at 40 Hz in coherence [25]. The presence of somatosensory feedback in bimanual upper arm flexion and extension also increases the neural coupling between muscles in the alpha and beta bands [26]. Task-dependent modulations of IMC in the 15-30 Hz range were also discovered during a ramping force generation versus force hold period study [27].

In addition, coherence analysis has also been employed to investigate the functional connectivity between the brain and muscles. Cortico-muscular coherence (CMC) analysis has been applied to magnetoencephalographic (MEG) and EMG data [28], which reported the CMC in 15-30 Hz to be related to hand motor function. A previous CMC study with electroencephalographic (EEG) and EMG recordings [20] reported the strongest cortico-muscular coupling strength in the beta frequency band (15-35 Hz) during upper limb movement. CMC and IMC in the beta band were also conducted concurrently during a two-finger pinch grip task with the first dorsal interosseus and abductor pollicis brevis in neurologically healthy individuals, and found that the beta band is indicative of a synergistic control of muscles where the coherent cortical areas functionally bind task-related motor neurons into functional units [29]. Overall, previous studies consistently suggest the alpha, beta, and gamma frequency bands are of importance in neuromuscular control and of different origins.

Muscle network analysis is a novel method that was recently developed to study the functional connectivity of muscles to further explain the property of neural inputs of muscle synergies and their capacity to simplify motor control [30]. Muscle networks are derived through the decomposition of EMG-EMG coherence to identify the shared frequencies at which certain muscles are co-modulated by some common neural input whereas muscle synergies are identified through decomposition of EMG-EMG amplitude to identify the sets of muscles co-active in motor task performance. Muscle synergies group together muscles based on the co-variation of EMG amplitude during force generation whereas muscle networks group together muscles based on their common neural input in distinct spectral regions, seen as the co-modulation of EMG frequencies, as assessed through the decomposition of the coherence. Previous studies have shown that muscle synergies and coherence muscle networks are complementary to each other and both necessary to understand neuromuscular motor control [30], [31]. Muscle networks have been studied in healthy individuals during postural tasks [30], [32] as well as gait analysis [31], but not yet in individuals with impaired motor control function such as stroke. Thus, how stroke alters muscle networks remains unknown even though the scientific findings can support a better understanding of the changes in intermuscular coordination as the severity of post-stroke impairment increases.

In this study, we performed muscle network analysis with the EMG data recorded during isometric force generation, for the first time, in post-stroke survivors of various impairment levels and age-matched healthy controls. We aimed to determine alterations in specific muscle network patterns in stroke and how the alterations would be associated with the severity of motor impairment after stroke. This study presents a re-analysis of existing datasets from Roh *et al.* [16], [17] with the new goal of identifying functional intermuscular connectivity of stroke patients through coherence and muscle network analysis.

II. Methods

A. Participants & Demographics

In total, twenty-six stroke survivors with either single hemorrhagic or ischemic stroke were recruited to participate in the study, which consists of eight mildly impaired (aged 55.6 $\pm$ 9.5 years), eight moderately impaired (aged 56.0 $\pm$ 8.7 years), [16] and ten severely impaired (aged 61.8 $\pm$ 10.0 years) stroke survivors. Six age-matched healthy participants (aged 63.2 $\pm$ 7.6 years) [17] were recruited as a healthy control group. Healthy participants were neurologically intact and possessed neither muscular nor orthopedic impairments of upper limbs. Clinical assessment (Fugl-Meyer (FM) assessment) was performed for the stroke survivors to measure motor impairment. Mildly impaired stroke patients recruited in this study had a mean FM score of 55.3 $\pm$ 5.3 (FM range: 50-66). Moderately impaired stroke patients had a mean FM score of 36.1 $\pm$ 7.0 (FM range: 29-45). Severely impaired stroke patients had a mean FM score of 17.5 $\pm$ 3.8 (FM range: 12-23). Surface electromyography (sEMG) signals were collected from the eight elbow and shoulder muscles of the affected limb in the stroke survivors and both limbs in healthy participants, respectively. For the details of the stroke survivor demographics and clinical scores, readers are referred to Roh's previous work published with the same data [17]. The study was performed in accordance with the Declaration of Helsinki, with the approval of the Northwestern University Institutional Review Board. Each participant gave informed consent before testing.

B. Data Acquisition

Hand position and 3D forces generated at the hand were recorded using the Multi-Axis Cartesian-based Arm Rehabilitation Machine (MACARM). The MACARM is a cable-robot designed for upper limb motor rehabilitation [33], [34]. Forces, arm orientation, and handle position were sampled at 64 Hz. Surface EMG signals were recorded (Bagnoli 8; Delsys, Boston, MA) from the eight elbow and shoulder muscles: brachioradialis (BRD), biceps brachii (BIm), triceps brachii, long and lateral heads (TRIlong & TRIlat, respectively), anterior, middle, and posterior deltoid fibers (AD, MD, PD, respectively), and pectoralis major (PECTclav). Surface EMG signals were amplified (x1000), online band-pass filtered (20-450 Hz), and sampled at 1920 Hz. The MACARM and sEMG amplifier were synchronized with a common clock and trigger for simultaneous data acquisition between them. Roh *et al.* previously indicated the following muscle pairs were synergistically activated in all four groups (healthy, mild-stroke, moderate-stroke, and severe-stroke groups): BRD-BIm, TRIlat-TRIlong, AD-MD, and MD-PD. Synergistic muscles exclusive to the healthy controls, mildly, and moderately impaired stroke patients were: AD-PECTclav and MD-PECTclav.

C. Experimental Design

Participants voluntarily generated forces under isometric conditions in a self-paced manner in fifty-four different directions distributed approximately uniformly in the three-dimensional force space while grasping the gimbaled handle of the MACARM with their hand in front of the ipsilateral shoulder. Throughout the task performance, the participant's arm remained stationary, and the forces were generated against the resistance of the handle of the MACARM. The large number of targets in multiple directions ensured robustness of the previous muscle synergy analysis by observing co-activation of muscles in a wider range of motion such that the results were not biased towards a specific direction. The target force magnitude was set at 40% maximum lateral force. A successful trial required for the participant to match a cursor on a computer monitor to a target sphere for at least 800 milliseconds by maintaining the almost same magnitude and direction of a force target (stable force generation period). Stroke patients performed the task with their affected limb while healthy controls performed the task with both arms. An inter-trial interval of 10 seconds and a 1-minute resting period were introduced to avoid muscle fatigue during task performance. All participants were right-hand dominant. For a more detailed explanation of the experimental design, readers are referred to our previous study [17].

D. Data Analysis

Trials in which individuals could not perform the force target matching were discarded from the analysis. The stable force generation phase of each successful trial was extracted. The EMG data was further demeaned, rectified using the Hilbert transform, and normalized to unit variance to prevent subsequent analyses to be biased by muscles with high variance [35], [36]. Signals from all successful trials were then concatenated in order to provide more samples for coherence analysis.

Magnitude-squared coherence is derived by calculating the cross-spectrum between two signals and normalizing it to the signals' auto-spectra (1), followed by the squared modulus [23], [24]. IMC was calculated via the magnitude-squared coherence for all twenty-eight muscle pairs among the eight upper-arm muscles. A Hanning window with a length of 500 milliseconds and 50% window overlap was applied and coherence was calculated in the frequency range of 0-50 Hz with a spectral resolution of 2 Hz [37].

$$C_{xy} = \frac{|P_{xy}|^2}{P_{xx} * P_{yy}} \tag{1}$$

A non-negative matrix factorization (NNMF) was applied to the coherence matrices to identify unique spectral patterns shared by the muscles [30]–[32]. A lower-rank approximation of IMC with weight coefficients (strength of muscle-pair contribution) and activation patterns (identified patterns in coherence) was achieved from NNMF. As a result, the coherence matrices were modeled as a k-ranked reconstruction matrix, M, with residual reconstruction error matrix E using NNMF. The reconstruction matrix M has the following dimensions: f (discrete frequencies evaluated), m (the total number of muscle pairs), and k (matrix rank). This resulted in two matrices, W and H (2). W and H are the coherence patterns and edge weights of the network, respectively.

$$M_{f*m} \approx (W_{f*k} * H_{k*m}) + E_{f*m} \tag{2}$$

Since the number of unique muscle networks needed to explain the force generation is unknown prior to analysis, variance accounted for (VAF) was used to determine the minimum number of spectral coherence patterns necessary to explain IMC with a threshold of 90% of VAF [38]. VAF indicates to what extent the outputs of NNMF can explain the total variance of the input data. VAF was calculated using the Frobenius norms of the error matrix E and reconstruction matrix M (3).

$$VAF = 1 - \frac{|E|^2_{fro}}{|M|^2_{fro}} \tag{3}$$

Coherence muscle networks were constructed after identifying the coherence patterns using NNMF. These activation patterns factorized from the coherence matrix represent the unique frequency patterns shared by sets of muscles during stable force generation. The weight coefficients are taken to be the undirected weighted functional connectivity matrices. First, coherence patterns were re-ordered across subjects per group. Then, coherence patterns extracted from NNMF were converted to unit vectors and the vector norm of these coherence patterns were used to re-scale the adjacency matrices such that the contribution of each subject to an average group network was further normalized. Muscle networks were visualized by thresholding the individual adjacency matrices to the top 30% of edge weights magnitude and averaging them across subjects within a group. Adjacency matrices and network topologies were plotted using uniform thresholds per group to facilitate

intergroup and intragroup comparisons of coherence muscle networks. Network edges were plotted as either low (0-33%), medium (33-67%), or high-strength (67-100%) depending on their relation to the maximal activation coefficient magnitude per group. Network visualization was aided using the Brain Connectivity Toolbox [39].

Coherence values were further normalized to Z-scores prior to statistical testing via the hyperbolic tangent transformation to facilitate statistical comparison across participants and groups [25], [29], where L is the number of segments used in the calculation of IMC (4).

$$Z = \frac{\tan^{-1}\left(\sqrt{C}_{xy}\right)}{\sqrt{1/(2L)}} \tag{4}$$

The means of IMC were statistically compared across synergistic muscle pairs (BRD-BIm, TRIlong-TRIlat, AD-MD, AD-PD, MD-PD, AD-PECTclav, and MD-PECTclav) in the alpha (8-13 Hz) band via balanced One-Way Analysis of Variance (ANOVA) with a pre-set alpha level of 0.05. ANOVA tests were conducted per muscle-pair and frequency band as no assumption was made concerning the dependence of one frequency band or muscle-pair to one another. The Benjamini-Hochberg correction was used to correct the false discovery rate across the multiple ANOVA tests. The means with significant differences identified from ANOVA after p-value adjustment were further analyzed with a multiple comparisons test using Tukey's Honestly Significant Difference Procedure. The p-values from multiple comparisons tests were accompanied by Hedges' g to demonstrate the effect sizes. Hedges' g is a corrected effect size value considering the number of samples in a group. Hedges' g was used to show the magnitude of difference between two groups in terms of standard deviations. All offline data processing was conducted using MATLAB (MATLAB R2017b, The MathWorks, Inc.).

III. Results

A. Stroke Alters Intermuscular Coherence

Stroke is associated with a decrease in the common neural input to muscles, as evidenced with a decrease in the magnitude of IMC. Fig. 1 shows the group averaged IMC for each muscle pair and sub-group. The most qualitatively distinguishable difference in the coherence patterns between healthy controls and stroke survivors were observed for the AD-MD, MD-PD, and TRIlat-TRIlong muscle pairs. These muscle pairs indicate greater magnitude of coherence overall versus the other muscle pairs in the coherence matrix. The magnitude of the coherence tended to be reduced in stroke survivors compared to healthy controls in these key muscle pairs.

The reduced magnitude of coherence associated with stroke was found to be statistically significant compared to the healthy controls. Average coherence values in the alpha band of synergistic muscle pairs were extracted and compared with balanced one-way ANOVA statistical tests for quantitative analysis following a hyperbolic tangent transformation. Table I reports the original and adjusted p-values for ANOVA test, mean and standard deviation of coherence per group for significant p-values, multiple-comparisons, and the Hedges' g value.

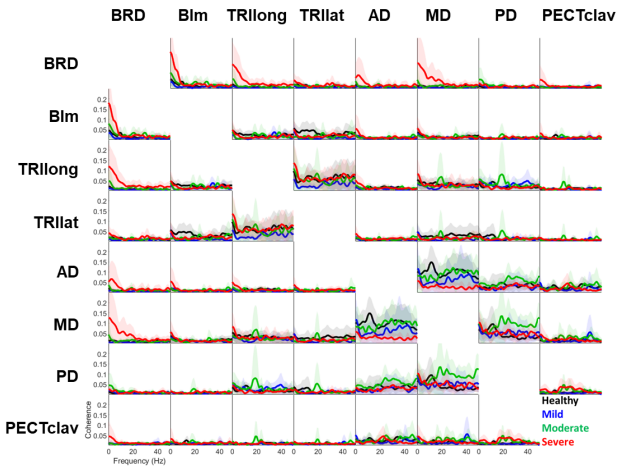

Fig. 1. Frequency-dependent intermuscular coherence averaged across the participants in each of the four sub-groups. Shaded regions indicate the 95% confidence interval for the group-averaged coherence spectra.

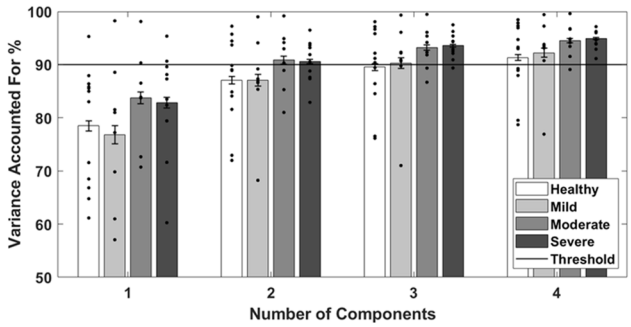

Fig. 2. Variance accounted for (VAF) by increasing the number of extracted spectral coherence patterns from one to four. The number of spectral coherence patterns is estimated as the one with at least 90% of the VAF. Stroke patients require fewer number of spectral coherence patterns to explain functional muscle connectivity.

The AD-MD muscle pair showed significant differences ($p = 0.0047$; $p_{corrected} = 0.0329$) in alpha-band IMC. Following this up with the Tukey-Kramer test revealed significant differences between the healthy controls and chronic severe stroke patients ($p = 0.0036$). While not significant ($p = 0.0510$), AD-MD did appear to show some trend of healthy controls possessing greater alpha-band coherence versus the mild stroke group in the multiple-comparisons.

B. Stroke Decreases Complexity of Coherence

Healthy controls exhibited distinct functional muscle association in four distinct spectral ranges (CON1-CON4) whereas post-stroke survivors showed reduced functional connectivity. Fig. 2 demonstrates the VAF values as a function of the number of spectral patterns identified from coherence. Error bars in Fig. 2 represent the standard error of the mean (SEM). The criterion for selecting the number of muscle networks was set to meet or exceed a 90% global VAF threshold. The minimum number of muscle networks, necessary to explain coherence data of each sub-group, was determined based on the variance of IMC accounted for (VAF) by the spectral coherence patterns extracted by NNMF. Mild-stroke patients exhibited functional connectivity in three spectral ranges (MIL1-MIL3). Moderate-stroke and severe-stroke patients were observed

TABLE I
MULTIPLE-COMPARISONS TESTS FOR NORMALIZED INTERMUSCULAR COHERENCE

ANOVA Tests				Alpha-Band Coherence			Multiple-Comparisons Tests			
Muscle-Pair	p-value	Rank	Adjusted p-value	Group	Mean	Deviation	Group 1	Group 2	p-value	Hedges' g
AD-MD	0.0047	1	0.0329	Healthy	7.1013	4.0383	Healthy	Mild	0.0510	1.0535
TRIlong-TRIlat	0.3117	2	0.7667	Mild	3.6893	2.1613	Healthy	Moderate	0.2175	0.7834
AD-PECTclav	0.3286	3	0.7667	Moderate	4.5984	2.0272	Healthy	Severe	0.0036	1.4569
BRD-BIm	0.5587	4	0.8484	Severe	2.6486	1.5410	Mild	Moderate	0.9132	0.4339
MD-PD	0.6536	5	0.8484				Mild	Severe	0.8585	0.5545
MD-PECTclav	0.8119	6	0.8484				Moderate	Severe	0.4602	1.0829
AD-PD	0.8484	7	0.8484							

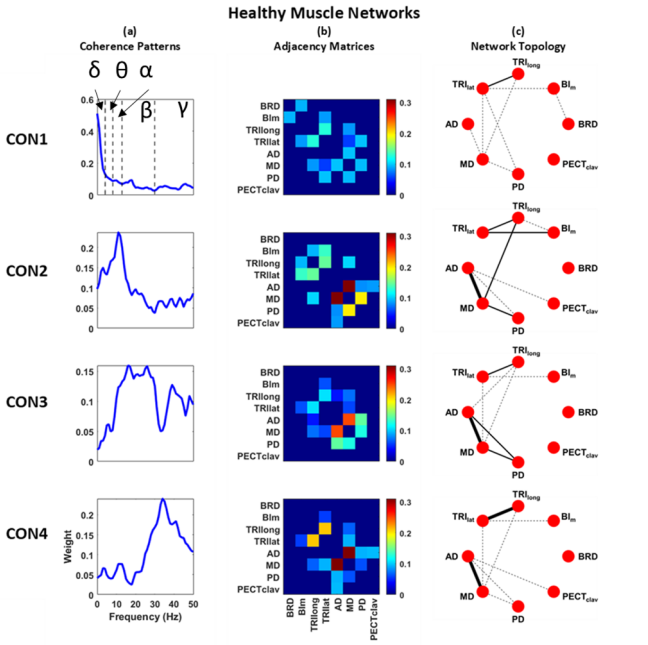

Fig. 3. Average muscle networks of the healthy group. Frequency limits for the delta, theta, alpha, beta, and gamma bands are presented with the CON1 network coherence pattern for an ease of interpretation with their Greek lettering scheme.

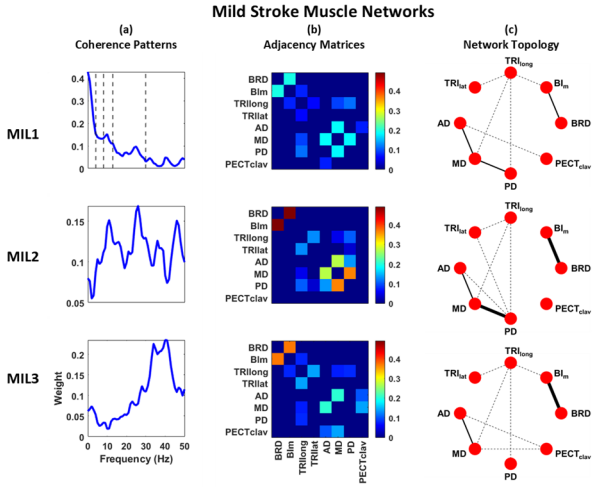

Fig. 4. Average muscle networks of the mild-stroke group.

to possess coherence patterns in only two spectral ranges (MOD1-MOD2 and SEV1-SEV2, respectively).

C. Muscle Network Topology

With the 90% global VAF as the threshold for selecting the appropriate number of muscle networks, four muscle networks were identified in healthy controls. Fig. 3a shows the four corresponding spectral coherence patterns, identified by NNMF in an increasing order of spectral content (low to high frequency), which are associated with the four weighted undirected adjacency matrices (Fig. 3b) thresholded to the top 30% of maximal activation coefficient magnitude. Each of the four muscle networks (Fig. 3c) corresponds to each specific spectral coherence patterns in Fig. 3a and adjacency matrices in Fig. 3b in the same row. Edge weights are plotted as "low" (dashed), "medium" (thin), and "high" (thick) strengths proportional to the maximum edge weight per group. Low, medium, and high strength edges indicate the lower third (0-33%), middle third (33-67%), and top third (67-100%) of the maximum activation coefficients across networks.

Healthy controls were found to have functional muscle connectivity in various well-defined frequency bands. The peak spectral contents of the four muscle networks (CON1-CON4) in the healthy group lie in different frequency bands: the delta band (CON1 network), theta and alpha bands (CON2 network), beta band (CON3 network), and gamma band (CON4 network).

Mild-stroke patients also indicated functional connectivity in different frequency bands but merging of some spectral patterns was noted. Like Fig. 3, Fig. 4 depicts the corresponding coherence patterns in Fig. 4a, adjacency matrices in Fig. 4b and muscle networks in Fig. 4c in mild-stroke patients (MIL1-MIL4). The muscle networks of the mild-stroke group seem to focus on combined delta and theta bands (MIL1 network), combined alpha and beta bands (MIL2 network), and the gamma band (MIL3 network).

Moderate and severe stroke groups were found to have the simplest functional connectivity with less defined spectral coherence patterns compared to the mild-stroke patients and healthy controls. Fig. 5 depicts the corresponding spectral coherence patterns, adjacency matrices, and muscle networks in moderate-stroke (MOD1-MOD2) and severe-stroke (SEV1-SEV2) patients, respectively. The coherence patterns extracted from stroke survivors with moderate impairment are much

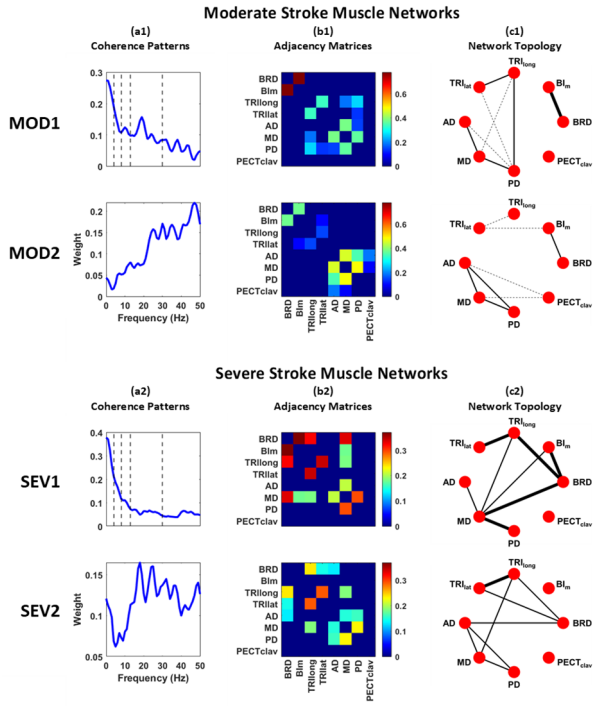

Fig. 5. Average muscle networks of the moderate-stroke and severe-stroke groups, respectively.

simpler in comparison to those of the healthy controls. The frequency content of the stroke muscle networks peaks in the combined delta, theta, and alpha bands for the MOD1 network and the combined beta and gamma bands for the MOD2 network. The coherence pattern associated with the SEV1 network peaks in the combined delta and theta bands. The SEV2 network is concentrated mostly in the beta band.

IV. Discussion

This study aimed to identify the post-stroke alterations in the intermuscular connectivity of upper limb muscles during isometric force generation using conventional coherence analysis and the novel muscle network analysis technique. Statistical analyses indicated that neurologically intact and less severely impaired post-stroke individuals possessed greater IMC in synergistic muscles, as compared to more severely impaired stroke survivors. The increase in post-stroke severity was associated with fewer functional muscle networks needed to explain the variance of IMC. The coherence muscle networks are mostly comprised of synergistic muscle pairs, showing that the frequency-based co-modulation of these synergistic muscles are vital in the muscle network composition. The coherence in alpha band, which is a spectral region of interest especially for IMC, noticeably decreased post-stroke, as evidenced by statistical analyses and muscle networks. Coherence patterns observed in stroke sub-groups showed a reduction in the magnitude of alpha-band coherence in mild- and moderate-stroke groups and a complete absence of any alpha-band peaks for the severe-stroke group. The consequences of the contralesional cortico-reticulospinal tract (RST) hyperexcitability and upregulation have been proposed to be associated with the emergence of abnormal muscle synergy patterns and disordered movement control after stroke [41]. Since the RST has several connections to synergistic muscles it can be assumed that the post-stroke RST hyperexcitability plays a role in the appearance of abnormal synergistic control. The absence or reduction of alpha band IMC may be explained by the role of RST hyperexcitability in conjunction with the abnormal synergistic control, since alpha-band coupling is due to some sub-cortical input to motor neuron pools.

Muscle networks can potentially provide valuable information in the stroke motor therapy and recovery process for motor-impaired individuals such as stroke patients. Results from this study indicate that muscle networks of different stroke severities do deviate from healthy controls. An increase in cortico-muscular coherence was observed by Pan *et al.* [42] during a combined electrical stimulation and motor training paradigm along with an increase in the FM score, so it is expected that improving the motor functions in post-stroke patients should improve the functional muscle connectivity seen in intermuscular coherence and coherence muscle networks.

The results of this study support the previous notion that anatomical muscle synergies and functional muscle networks are vital in the understanding of motor control and the role of the central nervous system in simplifying the motor control scheme [31]. Previous muscle network studies on neurologically intact individuals have identified a one-to-one mapping in the number of extracted motor modules and muscle networks [30], [31]. The results of these studies provided evidence to support the claim that stroke reduces the complexity of IMC as well as the number of muscle networks during motor task performance (or motor control).

It can be conjectured that the central nervous system is composed of multiple unique neural circuits, i.e. cortical inputs, which are connected to various sub-cortical units, and each neural circuit is responsible for the co-modulation of some muscles at some specific frequency range. The consequences of stroke on the brain induce neurological damage to some neural circuits, resulting in alterations in the strength of neuromuscular connectivity. This damage to the neural circuits in stroke is evidenced by the reduced magnitude of IMC among synergistic muscles. For example, healthy controls possessed one muscle network concerning the alpha band and another muscle network for the beta band and gamma band (CON2 and CON3 in Fig. 4, respectively). The mild-stroke group had one muscle network with coherence in the alpha, beta, and gamma bands together (MIL2 in Fig. 5). This spectral merging of physiologically relevant frequencies during neuromuscular control may be a result of the damage to the neural circuit responsible for alpha-band connectivity, potentially subcortical, perhaps spinal cord circuitries [25]. Moderate-stroke and severe-stroke groups present no distinguishable coherence peak in the alpha band, possibly indicating severe disruption to the specific neural circuit comprised of alpha-band connectivity.

A. Reduced Intermuscular Coherence Post Stroke

Synergistic muscles were found to be relevant in the coherence muscle networks, regardless of frequency content, in both

stroke and neurologically intact groups, which shows a strong link between large EMG amplitude correlations [31] and strong IMC during isometric force generation. Several synergistic muscle-pairs previously identified by Roh *et al.* appear to be highly coherent, such as TRIlat-TRIlong, AD-MD, and MD-PD. The synergistic AD-MD muscle pair demonstrated statistically significant differences in the mean of normalized coherence in the alpha-band frequencies, which suggests the overall decrease in shared neural input at those frequencies between muscles after stroke. Pizzamiglio *et al.* discovered an increase in high-frequency coherence (∼40-100 Hz) in certain muscle connections during the use of robot-assisted motor adaption and dynamic force generation, showing that the functional connectivity of muscles can be altered with specific motor training [43]. This work also supports the application of using muscle networks to track the improvement of functional muscle connectivity pre- and post-training for stroke patients. Functional coupling assessment of synergistic muscles may be used as a reliable biomarker in stroke motor recovery and assessment.

The results of the statistical difference of normalized coherence between healthy controls and severe-stroke patients are also congruent with the results from previous studies on assessing motor task performance of severe-stroke patients with upper-arm IMC in reaching tasks. Kisiel-Sajewicz *et al.* found significantly lower coherence for two synergistic muscles in upper-arm reaching, the anterior deltoid and triceps muscles, in the 0-11 Hz spectral range [18] post-stroke. The statistical tests from this study identified reduced alpha-band coherence between the two synergist muscles anterior and middle deltoids in the alpha band (8-13 Hz). Similarly, Chen *et al.* identified reduced gamma-band coherence in stroke patients between the ipsilateral flexor digitorum superficialis (FDS) and the contracting biceps of the impaired side during motor control [37]. These results indicate that stroke is associated with a significant reduction in functional muscle connectivity in synergistic muscles seen in voluntary movements, i.e., less voluntary control.

B. Fewer Muscle Networks Post Stroke

The current study demonstrated that, while four muscle networks were necessary to account for the variance of coherence patterns in healthy controls, only three muscle networks were needed to explain the variance of coherence patterns for the same task in the mild-stroke group, and two muscle networks were needed for both moderate-stroke and severe-stroke groups. The increase in severity of stroke impairment is accompanied by the decrease in functional coupling in the upper arm muscles, indicating a simplified functional control scheme. Roh *et al.* previously observed four muscle synergies needed to explain the muscle activation patterns for both healthy and all stroke groups [16], [17]. It is noteworthy that although the number of muscle synergies was the same across all four groups, the functional coupling of those synergies defined in the frequency domain did change along with the anatomical intermuscular coordination. Synergistic muscles co-activated during stable force generation in time were also confirmed to be functionally associated with each other in different frequency bands via IMC. Typically, in healthy controls, the muscle pairs with strong functional connectivity in each muscle network were synergistic muscles (Fig. 3). For example, the BRD-BIm pair formed a low-strength edge in the CON1 network (Fig. 4). Synergistic muscle pairs of AD-MD and MD-PD were also observed in the CON1 network as low-strength edges whereas TRIlat-TRIlong was found as a medium-strength edge. The synergistic muscle pair AD-PECTclav was observed as a low-strength edge in the CON2 and CON4 networks. The synergistic AD-MD muscle pair appeared as high-strength edges in the CON2, CON3, and CON4 networks while the TRIlat-TRIlong muscle pair was also found as a high-strength edge in the CON4 network.

The current study showed that spectral merging of coherence patterns could act as one of the mechanisms of the decrease in the number of muscle networks in the three stroke sub-groups. In the mild-stroke group, the MIL2 muscle network coherence pattern presents two distinct peaks in the alpha and beta bands, whereas the MIL1 and MIL3 networks represented functional connectivity in the delta and gamma bands, respectively (Fig. 5). Considering that fractionation and merging of muscle synergies have been reported as potential mechanisms of alterations in anatomical intermuscular coordination after stroke [13], [14], [44], it is possible that the functional muscle connections in the alpha and beta bands merged after stroke due to the neurological consequences of stroke. The synergistic muscle pair of BRD-BIm was found to be a medium-strength edge in the MIL1 network and as a high-strength edge for the MIL2 and MIL3 networks (Fig. 5), which was not observed in the healthy muscle networks. In both moderate-stroke and severe-stroke groups, further simplified functional connectivity was observed, and synergistic muscle pairs still consisted of the associated muscle networks in those groups. All synergistic muscles previously identified by Roh *et al.*, which comprised unique motor modules for the moderate-stroke and severe-stroke groups, were present in the MOD2 and SEV2 networks, respectively.

Another observation regarding muscle networks involved with lower frequency content (CON1, MIL1, MOD1, and SEV1) is that the number of medium-strength and high-strength edges increases as the severity of post-stroke motor impairment increases (Figs. 4-6). Only one medium-strength edge is present in the CON1 network whereas every other network connection is of low-strength. The MIL1 network presents with three medium-strength edges. The MOD1 network consists of four medium-strength edges and one high-strength edge and the SEV1 network is comprised of three medium-strength edges, five high-strength edges, and no low-strength edges whatsoever.

The current study suggests that stroke simplifies the functional motor control scheme. In healthy controls, the functional connectivity was easily separated into various well-defined frequency bands. In contrast, stroke patients exhibited functional connectivity in less well-defined frequency limits with a decrease in the coherence magnitude in higher frequency bands, commonly associated with sensorimotor tasks such as alpha and beta bands [18], [29]. The lower number of muscle

networks observed in stroke patients suggests that not only muscle coordination [17] but also the functional coupling between muscles is altered during isometric force generation. Thus, we reason that inducing the increase of coherence within these higher frequency bands can be key in successful motor rehabilitation post stroke.

According to Kerkman *et al.* it seems likely that IMC at very low frequencies such as the delta band identifies the covariation of rectified EMG envelopes that are crucial in muscle synergy analysis [31]. Indeed, synergistic muscles were identified in coherence muscle networks with lower spectral content for both healthy controls and all stroke impairment groups (CON1, MIL1, MOD1, and SEV1, respectively; Figs. 4-6). Additionally, it was conjectured that muscle networks associated with higher IMC content might in fact be isolating different functional pathways of the neuromuscular system [31].

Besides the delta-band coherence, a beta-band and gamma-band coherence pattern was consistently observed across healthy controls and the three stroke sub-groups (CON3, MIL2, MOD2, and SEV2, respectively; Figs. 3–5). Considering beta-band coherence is known to play a role in the maintenance of isometric force [25], [27], [45], [46], the beta-band coherence pattern would be consistently observed across all participant groups potentially due to the motor task constraints performed in the current study. Also, during force generation, beta-band coherence can be reflective of a synergistic control strategy in which the cortex binds task-related motor neurons into functional units [27], [29], [47]–[50]. This finding is congruent with the idea that functionally related muscles share a common intermuscular beta-band input [27], [46] whose origin would be the motor cortex for such beta-band drive [47]. If the beta-band coherence pattern would reflect the cortical binding of muscles as suggested in previous studies [49], [50], we reason that this beta-band coherence pattern would favor more synergistic intermuscular coordination. Overall, it would be conceivable to reason that, as the severity of motor impairment increased after stroke, the greater number of muscle pairs with stronger connectivity edges in the muscle networks of the beta-band and gamma-band coherence pattern was observed, which could reflect the inability or reduced capability of cortical neural input to activate muscles in isolation during isometric force generation.

It is possible that cortical and or sub-cortical damage induced by stroke impairs the neural input to the upper arm and elbow muscles in higher frequency bands by altering the corticospinal pathways, which results in a simpler functional control scheme to compensate for lower efficiency in neuromuscular control. The absence of unique coherence patterns in higher frequency bands in stroke patients is evidence of some alterations in the common cortico-spinal input to motor neurons. Since functional connectivity seems to be highly affected by the anatomical muscle networks, as suggested by Kerkman *et al.*, it is conceivable to reason that the alteration in muscle co-activation and anatomical intermuscular coordination after stroke ultimately influences the change in magnitude and morphology of IMC.

C. Study Limitations

The current study could be further improved on in later studies by addressing the following points. Intermuscular coherence was calculated in this study by concatenating data from several target directions in an isometric force generation task. Additionally, while all healthy controls were able to generate force in all target directions some stroke patients were not able to generate force in certain target directions, resulting in an unequal number of trials per subject. The average intermuscular coherence of one group may differ from another group not only by neurological health but also by the number of target directions which the subjects were able to perform. Coherence muscle networks in the stroke population should be re-assessed in a paradigm which includes less variance in the target direction of force generation. Also, while coherence networks were determined through NNMF decomposition on a subject-specific basis not every decomposition will yield the same coherence patterns. It may be beneficial to update the muscle network method in a future study such that NNMF decomposition is not necessary to create the adjacency matrix.

V. Conclusion

Using novel muscle network analysis to assess the functional co-modulation of muscles, it was shown that post-stroke survivors exhibit differences in functional muscle connectivity during stable force generation as compared to healthy controls. Statistically significant reductions in IMC of synergistic deltoid muscles were identified at alpha-band frequencies between healthy controls and stroke patients of severe impairment. A reduced number of muscle networks were identified for increased severity of stroke impairment. Synergistic muscles in stable force generation were found to be key nodes in muscle networks. Understanding the underlying neural input to muscles in post-stroke survivors can prove vital in improving motor rehabilitation by identifying the abnormal nodes in the muscle networks and targeting them heavily in the motor rehabilitation process.

References

[1] E. J. Benjamin *et al.*, "Heart disease and stroke statistics—2019 update: A report from the American heart association," *Circulation*, vol. 139, no. 10, pp. e56–e528, 2019.
[2] T. E. Twitchell, "The restoration of motor function following hemiplegia in man," *Brain*, vol. 74, no. 4, pp. 443–480, 1951.
[3] S. Brunnstrom, H. J. Hislop, and P. Carson, *Movement Therapy in Hemiplegia: A Neurophysiological Approach*. Philadelphia, PA, USA: Harper & Row, 1970.
[4] J. P. A. Dewald, P. S. Pope, J. D. Given, T. S. Buchanan, and W. Z. Rymer, "Abnormal muscle coactivation patterns during isometric torque generation at the elbow and shoulder in hemiparetic subjects," *Brain*, vol. 118, no. 2, pp. 495–510, 1995.
[5] E. Bizzi, F. Mussa-Ivaldi, and S. Giszter, "Computations underlying the execution of movement: A biological perspective," *Science*, vol. 253, no. 5017, pp. 287–291, Jul. 1991.
[6] A. d'Avella, P. Saltiel, and E. Bizzi, "Combinations of muscle synergies in the construction of a natural motor behavior," *Nature Neurosci.*, vol. 6, no. 3, pp. 300–308, Mar. 2003.
[7] G. Torres-Oviedo, J. M. Macpherson, and L. H. Ting, "Muscle synergy organization is robust across a variety of postural perturbations," *J. Neurophysiol.*, vol. 96, no. 3, pp. 1530–1546, Sep. 2006.
[8] E. Bizzi, V. C. K. Cheung, A. d'Avella, P. Saltiel, and M. Tresch, "Combining modules for movement," *Brain Res. Rev.*, vol. 57, no. 1, pp. 125–133, Jan. 2008.

[9] C. B. Hart and S. F. Giszter, "A neural basis for motor primitives in the spinal cord," *J. Neurosci.*, vol. 30, no. 4, pp. 1322–1336, Jan. 2010.

[10] E. Bizzi and V. C. K. Cheung, "The neural origin of muscle synergies," *Frontiers Comput. Neurosci.*, vol. 7, p. 51, Apr. 2013.

[11] L. H. Ting *et al.*, "Neuromechanical principles underlying movement modularity and their implications for rehabilitation," *Neuron*, vol. 86, no. 1, pp. 38–54, Apr. 2015.

[12] V. C. K. Cheung, L. Piron, M. Agostini, S. Silvoni, A. Turolla, and E. Bizzi, "Stability of muscle synergies for voluntary actions after cortical stroke in humans," *Proc. Nat. Acad. Sci. USA*, vol. 106, no. 46, pp. 19563–19568, Nov. 2009.

[13] V. C. K. Cheung *et al.*, "Muscle synergy patterns as physiological markers of motor cortical damage," *Proc. Nat. Acad. Sci. USA*, vol. 109, no. 36, pp. 14652–14656, Sep. 2012.

[14] D. J. Clark, L. H. Ting, F. E. Zajac, R. R. Neptune, and S. A. Kautz, "Merging of healthy motor modules predicts reduced locomotor performance and muscle coordination complexity post-stroke," *J. Neurophysiol.*, vol. 103, no. 2, pp. 844–857, Feb. 2010.

[15] S. W. Lee, K. Triandafilou, B. A. Lock, and D. G. Kamper, "Impairment in task-specific modulation of muscle coordination correlates with the severity of hand impairment following stroke," *PLoS ONE*, vol. 8, no. 7, Jul. 2013, Art. no. e68745.

[16] J. Roh, W. Z. Rymer, E. J. Perreault, S. B. Yoo, and R. F. Beer, "Alterations in upper limb muscle synergy structure in chronic stroke survivors," *J. Neurophysiol.*, vol. 109, no. 3, pp. 768–781, Feb. 2013.

[17] J. Roh, W. Z. Rymer, and R. F. Beer, "Evidence for altered upper extremity muscle synergies in chronic stroke survivors with mild and moderate impairment," *Frontiers Hum. Neurosci.*, vol. 9, p. 6, Feb. 2015.

[18] K. Kisiel-Sajewicz *et al.*, "Weakening of synergist muscle coupling during reaching movement in stroke patients," *Neurorehabil. Neural Repair*, vol. 25, no. 4, pp. 359–368, May 2011.

[19] K. M. Fisher, B. Zaaimi, T. L. Williams, S. N. Baker, and M. R. Baker, "Beta-band intermuscular coherence: A novel biomarker of upper motor neuron dysfunction in motor neuron disease," *Brain*, vol. 135, no. 9, pp. 2849–2864, Sep. 2012.

[20] Y. Gao, L. Ren, R. Li, and Y. Zhang, "Electroencephalogram—Electromyography coupling analysis in stroke based on symbolic transfer entropy," *Frontiers Neurol.*, vol. 8, p. 716, Jan. 2018.

[21] D. D. Lee and H. S. Seung, "Learning the parts of objects by non-negative matrix factorization," *Nature*, vol. 401, no. 6755, pp. 788–791, Oct. 1999.

[22] X. Li, Y. Du, C. Yang, W. Qi, and P. Xie, "Merging of synergistic muscles and intermuscular coherence predict muscle coordination complexity," in *Proc. IEEE Int. Conf. Inf. Automat. (ICIA)*, Aug. 2016, pp. 791–795.

[23] J. R. Rosenberg, D. M. Halliday, P. Breeze, and B. A. Conway, "Identification of patterns of neuronal connectivity—Partial spectra, partial coherence, and neuronal interactions," *J. Neurosci. Methods*, vol. 83, no. 1, pp. 57–72, Aug. 1998.

[24] D. M. Halliday and J. R. Rosenberg, "On the application, estimation and interpretation of coherence and pooled coherence," *J. Neurosci. Methods*, vol. 100, nos. 1–2, pp. 173–174, Jul. 2000.

[25] C. M. Laine and F. J. Valero-Cuevas, "Intermuscular coherence reflects functional coordination," *J. Neurophysiol.*, vol. 118, no. 3, pp. 1775–1783, Sep. 2017.

[26] H. B. Nguyen, S. W. Lee, M. L. Harris-Love, and P. S. Lum, "Neural coupling between homologous muscles during bimanual tasks: Effects of visual and somatosensory feedback," *J. Neurophysiol.*, vol. 117, no. 2, pp. 655–664, Feb. 2017.

[27] J. M. Kilner, S. N. Baker, S. Salenius, V. Jousmäki, R. Hari, and R. N. Lemon, "Task-dependent modulation of 15-30 Hz coherence between rectified EMGs from human hand and forearm muscles," *J. Physiol.*, vol. 516, no. 2, pp. 559–570, Apr. 1999.

[28] J. M. Kilner, S. N. Baker, S. Salenius, R. Hari, and R. N. Lemon, "Human cortical muscle coherence is directly related to specific motor parameters," *J. Neurosci.*, vol. 20, no. 23, pp. 8838–8845, Dec. 2000.

[29] A. Reyes, C. M. Laine, J. J. Kutch, and F. J. Valero-Cuevas, "Beta band corticomuscular drive reflects muscle coordination strategies," *Frontiers Comput. Neurosci.*, vol. 11, p. 17, Apr. 2017.

[30] T. W. Boonstra, A. Danna-Dos-Santos, H.-B. Xie, M. Roerdink, J. F. Stins, and M. Breakspear, "Muscle networks: Connectivity analysis of EMG activity during postural control," *Sci. Rep.*, vol. 5, no. 1, pp. 1–14, Nov. 2016.

[31] J. N. Kerkman, A. Bekius, T. W. Boonstra, A. Daffertshofer, and N. Dominici, "Muscle synergies and coherence networks reflect different modes of coordination during walking," *Frontiers Physiol.*, vol. 11, p. 751, Jul. 2020.

[32] J. N. Kerkman, A. Daffertshofer, L. L. Gollo, M. Breakspear, and T. W. Boonstra, "Network structure of the human musculoskeletal system shapes neural interactions on multiple time scales," *Sci. Adv.*, vol. 4, no. 6, Jun. 2018, Art. no. eaat0497.

[33] D. Mayhew, B. Bachrach, W. Z. Rymer, and R. F. Beer, "Development of the MACARM—A novel cable robot for upper limb neurorehabilitation," in *Proc. 9th Int. Conf. Rehabil. Robot. (ICORR)*, Jun. 2005, pp. 299–302.

[34] R. Beer, D. Mayhew, C. Bredfeldt, and B. Bachrach, "Technical evaluation of the MACARM: A cable robot for upper limb neurorehabilitation," in *Proc. 2nd IEEE RAS EMBS Int. Conf. Biomed. Robot. Biomechatronics*, Oct. 2008, pp. 942–947.

[35] L. J. Myers *et al.*, "Rectification and non-linear pre-processing of EMG signals for cortico-muscular analysis," *J. Neurosci. Methods*, vol. 124, no. 2, pp. 157–165, Apr. 2003.

[36] T. W. Boonstra and M. Breakspear, "Neural mechanisms of intermuscular coherence: Implications for the rectification of surface electromyography," *J. Neurophysiol.*, vol. 107, no. 3, pp. 796–807, Feb. 2012.

[37] Y.-T. Chen, S. Li, E. Magat, P. Zhou, and S. Li, "Motor overflow and spasticity in chronic stroke share a common pathophysiological process: Analysis of within-limb and between-limb EMG-EMG coherence," *Frontiers Neurol.*, vol. 9, p. 795, Oct. 2018.

[38] T. Wojtara, F. Alnajjar, S. Shimoda, and H. Kimura, "Muscle synergy stability and human balance maintenance," *J. Neuroeng. Rehabil.*, vol. 11, no. 1, p. 129, 2014.

[39] M. Rubinov and O. Sporns, "Complex network measures of brain connectivity: Uses and interpretations," *NeuroImage*, vol. 52, no. 3, pp. 1059–1069, Sep. 2010.

[40] M. Jesunathadas, J. Laitano, T. M. Hamm, and M. Santello, "Across-muscle coherence is modulated as a function of wrist posture during two-digit grasping," *Neurosci. Lett.*, vol. 553, pp. 68–71, Oct. 2013.

[41] S. Li, Y.-T. Chen, G. E. Francisco, P. Zhou, and W. Z. Rymer, "A unifying pathophysiological account for post-stroke spasticity and disordered motor control," *Frontiers Neurol.*, vol. 10, p. 468, May 2019.

[42] L.-L.-H. Pan *et al.*, "Effects of 8-week sensory electrical stimulation combined with motor training on EEG-EMG coherence and motor function in individuals with stroke," *Sci. Rep.*, vol. 8, no. 1, pp. 1–10, Dec. 2018.

[43] S. Pizzamiglio, M. De Lillo, U. Naeem, H. Abdalla, and D. L. Turner, "High-frequency intermuscular coherence between arm muscles during robot-mediated motor adaptation," *Frontiers Physiol.*, vol. 7, p. 668, Jan. 2017.

[44] Y. Hashiguchi *et al.*, "Merging and fractionation of muscle synergy indicate the recovery process in patients with hemiplegia: The first study of patients after subacute stroke," *Neural Plasticity*, vol. 2016, pp. 1–7, Oct. 2016.

[45] A. Pogosyan, L. D. Gaynor, A. Eusebio, and P. Brown, "Boosting cortical activity at beta-band frequencies slows movement in humans," *Current Biol.*, vol. 19, no. 19, pp. 1637–1641, Oct. 2009.

[46] T. D. Aumann and Y. Prut, "Do sensorimotor β-oscillations maintain muscle synergy representations in primary motor cortex?" *Trends Neurosci.*, vol. 38, no. 2, pp. 77–85, Feb. 2015.

[47] T. W. Boonstra, "The potential of corticomuscular and intermuscular coherence for research on human motor control," *Frontiers Hum. Neurosci.*, vol. 7, p. 855, Dec. 2013.

[48] P. Brown, S. F. Farmer, D. M. Halliday, J. Marsden, and J. R. Rosenberg, "Coherent cortical and muscle discharge in cortical myoclonus," *Brain*, vol. 122, no. 3, pp. 461–472, Mar. 1999.

[49] C. M. Gray, "Synchronous oscillations in neuronal systems: Mechanisms and functions," *J. Comput. Neurosci.*, vol. 1, nos. 1–2, pp. 11–38, Jun. 1994.

[50] R. Balasubramanian and V. J. Santos, "The human hand as an inspiration for robot hand development," in *The Human Hand as an Inspiration for Robot Hand Development*. Cham, Switzerland: Springer, 2014, pp. 23–48.